JOURNAL OF MATERIALS SCIENCE 23 (1988) 2273–2280

# Special features of the formation of the diffusion bonded joints between copper and aluminium

F. A. CALVO, A. UREÑA, J. M. GOMEZ DE SALAZAR, F. MOLLEDA
*Department of Materials Science and Metallurgical Engineering, Faculty of Chemical Science, University Complutense of Madrid, Spain*

A metallographic study of diffusion bonds between aluminium and copper has been made in order to further understanding of the mechanism of bond formation for joints between dissimilar metals that form intermediate phases or intermetallic compounds. A three-stage mechanistic model based upon sintering principles has been proposed to explain this kind of diffusion joint.

## 1. Introduction

Dissimilar metal joints obtained by diffusion bonding are of great interest because diffusion bonding can avoid many of the difficulties which arise in fusion welding of two different metals if they are metallurgically incompatible. Obviously, not all the problems are solved by diffusion welding. One of the problems which appears in this type of joint is the formation of intermediate phases or intermetallic compounds in the bond. These compounds are often brittle, and their formation and growth reduce the mechanical properties of the joints. Because of this, in order to assess the mechanical behaviour of these joints, it is necessary to know the metallurgy of the joint formation, the nature of the intermetallic compounds, the kinetics of their formation, and the properties of these compounds or phases.

In this study we have experimented with diffusion bonding of aluminium and copper, metals which do not have complete solubility in the solid state, and form several phases and intermetallic compounds (Fig. 1). Our purpose was to study the metallurgical phenomena in the bond formation.

Several investigators have already proposed experimental or theoretical models, in order to explain the bonding; however, the majority of these models have been developed from homogeneous joints (between similar metals). For this reason, these models do not consider the peculiarities of the systems formed by dissimilar metals.

Metallography has been the fundamental technique used to develop an experimental model for the formation of aluminium–copper diffusion joints. These were studied by optical and scanning electron microscopy

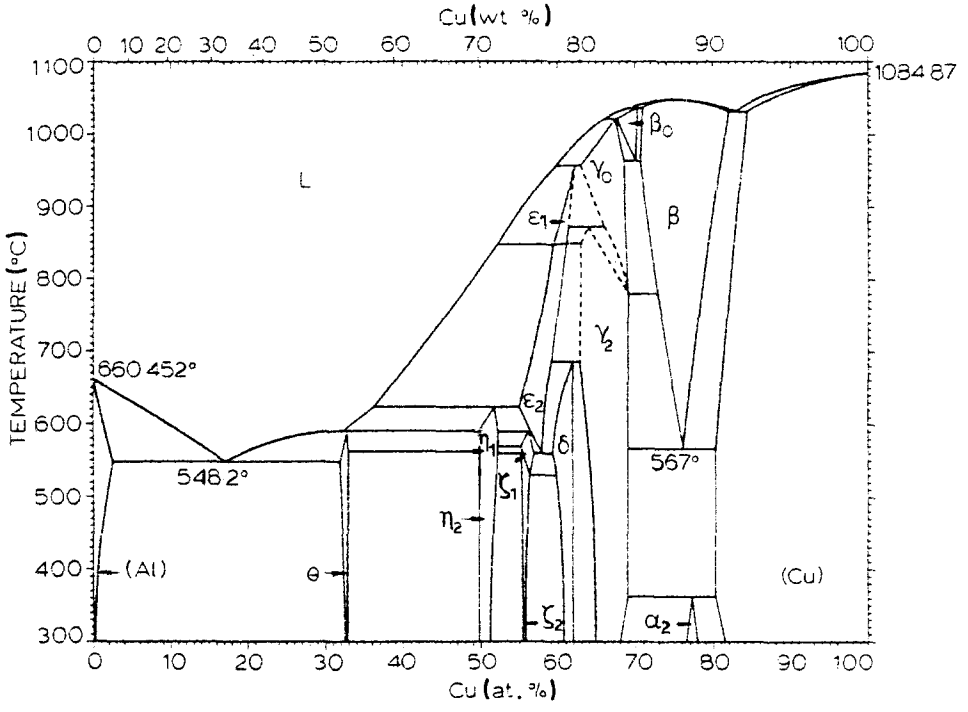


*Figure 1* Aluminium–copper phase diagram [1].

0022–2461/88 $03.00 + .12 

TABLE I Chemical composition of the base metals (wt %)

| | | | | | | | |
|---|---|---|---|---|---|---|---|
| C1100 | Pb | Fe | Ni | S | O | P | Cu |
| | 0.004 | 0.007 | 0.005 | 0.002 | 0.04 | – | Bal. |
| 1050 | Fe | Mn | Ni | Zn | Ti | Si | Al |
| | 0.4 | 0.02 | 0.03 | 0.01 | < 0.01 | 0.05 | Bal. |

(SEM), and the diffusion zones were analyzed by energy dispersive spectrometry (EDS) microanalysis and X-ray diffraction.

## 2. Experimental procedure

### 2.1. Experimental diffusion bonding unit

The equipment used to carry out the diffusion bonding experiments is similar to that used by us in the diffusion bonding of iron–copper [2]. Bonding temperature was measured by a chromel–alumel thermocouple spot-welded close to bond interface.

### 2.2. Base materials and sample preparation

Base metals used in the present work were 1050 aluminium and C11000 copper. Their chemical compositions are given in Table I.

Cylindrical samples, 15 mm diameter and 10 mm long, were used. The joining surfaces were finished on 600 grade emery paper, and cleaned with acetone in an ultrasonic bath just before bonding. However, this surface preparation does not prevent the formation of an aluminium oxide layer which plays an important role in the joint formation.

### 2.3. Bonding procedure and metallographic preparation

The bonding conditions (pressure, temperature and time) varied between 0.25 and 1.60 MPa, 400 and 520° C and 0.25 and 289 h, respectively, as is shown in Tables II and Table III. The experiments were performed in vacuum ($10^{-4}$ to $10^{-5}$ Pa).

Samples were heated to bonding temperature at approximately 0.65° C $sec^{-1}$ and slowly cooled ($\approx$ 0.25° C $sec^{-1}$), inside the vacuum chamber, under no load. The bonded samples were cut across the bonding surface and prepared for metallographic study.

Metallographic observations were made on polished samples. However, in some cases, thermal etching was used to improve the contrast between the different phases. Observation with polarized light clearly shows the crystalline structure of the intermetallic compounds. The great stability of these compounds reduces resistance to chemical or electrolytic etching.

TABLE II Diffusion bonding trials between aluminium and copper for different bonding pressures

| Sample | Temperature (° C) | Time (min) | Pressure (MPa) |
|---|---|---|---|
| P1 | 520 | 15 | 0.25 |
| P2 | 520 | 15 | 0.50 |
| P3 | 520 | 15 | 1.00 |
| P4 | 520 | 15 | 1.60 |
| P5 | 520 | 30 | 1.60 |

## 3. Results and discussion

### 3.1. Metallurgical mechanisms of joint formation

Some authors (e.g. Derby and Wallach [3], King and Owczarski [4], Garmong *et al.* [5] and Bartle [6]), have proposed several models to explain the formation processes of diffusion-bonded unions. However, these mechanistic models do not consider all the peculiarities that the aluminium–copper union presents. In copper/aluminium joint these are: (i) the existence of a coherent, continuous and stable aluminium oxide film on the aluminium surface, (ii) the possibility of formation of various intermediate phases or intermetallic compounds. Therefore, the proposed model must include both what happens with the aluminium oxide film and how the phases and compounds at the joint are formed. Final joining is obtained through three stages. In each stage, one or more mechanisms that are controlled by a bonding variable, will be dominant. This model is presented in Fig. 2.

#### *3.1.1. First stage*

The first stage of the joint formation might be called the "contact stage". It begins with the contact setting between the metallic surfaces at room temperature. In this stage the initial contact area is a small fraction of the theoretical or nominal area (Fig. 2a).

In essence, the first stage of bonding is dominated by yield and creep deformation mechanisms, in addition to the oxide film fracture mechanism.

At room temperature, the initial contact between the surfaces depends on the applied pressure and the compressive yield stress of both metals. A plastic deformation takes place in the contact points between microasperities which produces an increase in the contact area (Fig. 2b).

However, the presence of an oxide film (aluminium oxide) will interfere with the diffusion processes and,

TABLE III Diffusion bonding trials between aluminium and copper for long diffusion times

| Sample | Temperature (° C) | Time (h) | Pressure (MPa) |
|---|---|---|---|
| M1 | 400 | 42 | 1.00 |
| M2 | 400 | 121 | 1.00 |
| M3 | 400 | 169 | 1.00 |
| M4 | 400 | 289 | 1.00 |
| M5 | 440 | 72 | 1.00 |
| M6 | 440 | 100 | 1.00 |
| M7 | 440 | 129 | 1.00 |
| M8 | 440 | 144 | 1.00 |
| M9 | 480 | 16 | 1.00 |
| M10 | 480 | 36 | 1.00 |
| M11 | 480 | 44 | 1.00 |
| M12 | 480 | 64 | 1.60 |

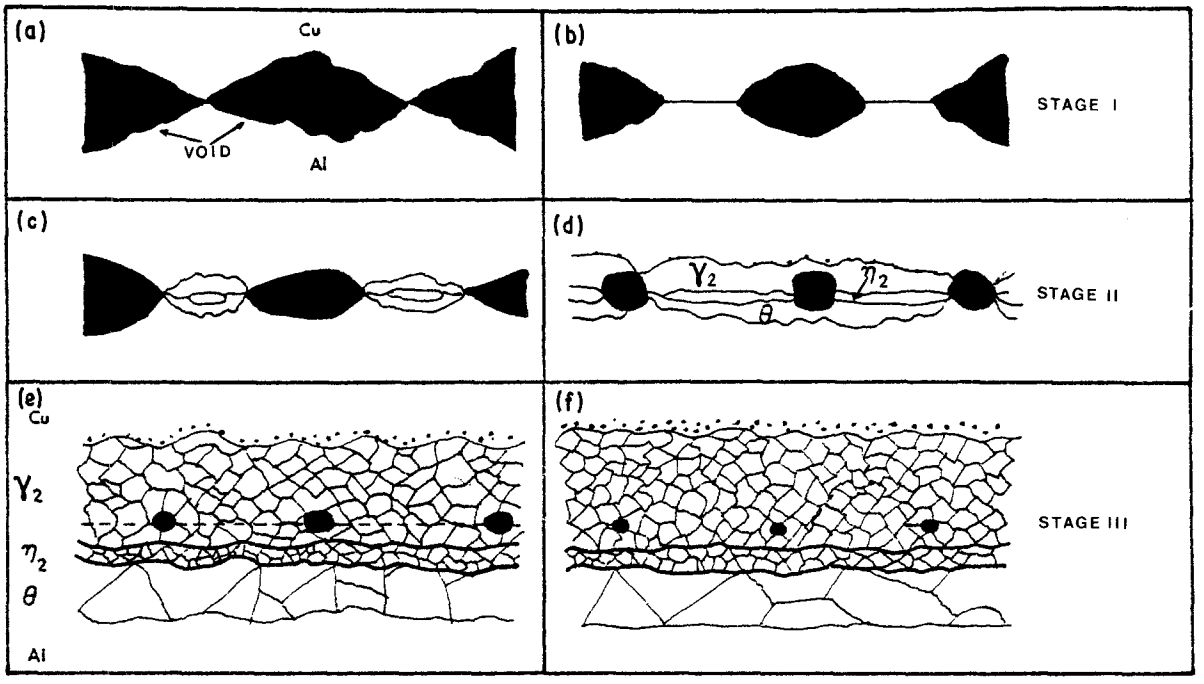


*Figure 2* Schematic diagram to illustrate the formation of an aluminium–copper diffusion joint. (a) Original contact surface between microasperities. (b) Growth of the contact area due to yield and creep deformation mechanisms. (c), (d) formation and growth of the first intermetallic compound nuclei, with spheroidization and shrinkage of interfacial voids. (e) Intermetallic compound layers growing parallel to the bond interface. (f) Migration of the bond interface from the original plane during $\tau_2$ grain growth.

consequently, the formation of an intimate contact between copper and aluminium.

Bryant [7] has classified the metal oxide films according to their influence on diffusion bonding, as a function of the solubility of oxygen in the metals and the standard energy of oxide formation ($\Delta G^0$). Bryant proved that metals with standard free energy values lower than $-350$ k cal mol$^{-1}$ and low solubilities present greater difficulty in achieving a diffusion bond. Aluminium was classified in this group, because of its large free energy of oxide formation ($-365$ cal mol$^{-1}$) and to the oxygen solubility (0.005 atm % for $T/T_m = 0.5$). Therefore, diffusion bonding of aluminium and copper presents a great difficulty, and the oxide film must be broken before the necessary intimate between both metals can be obtained.

Several diffusion bonding tests between copper and aluminium were performed under different conditions (Table II), in order to determine the mechanisms that participate in this first stage and the role played by the bonding pressure in the joint process. These experiments were carried out at constant temperature (520° C) and time (15 min), varying the bonding pressure between 0.25 and 1.60 MPa.

An increase of the bonding pressure produced an increase of the initial contact between both metals.

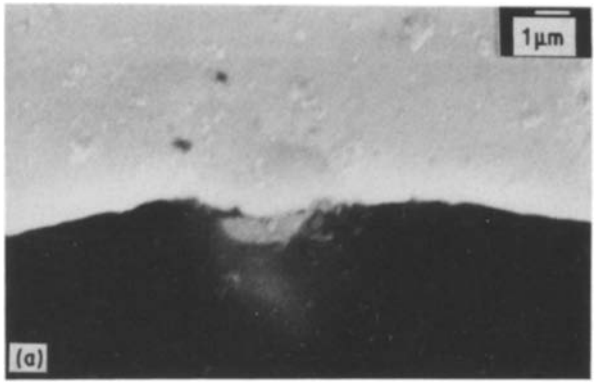


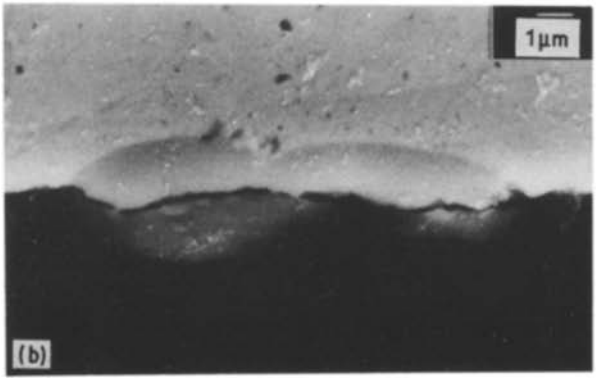


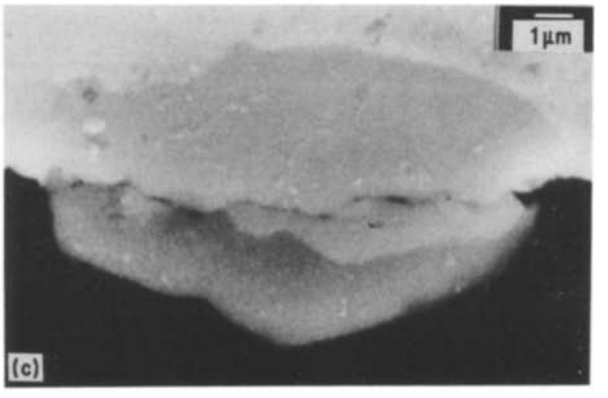


*Figure 3* Different growth stages of the first nuclei of intermetallic compounds, due to the increase of bonding pressure. (a) 0.25 MPa; (b) 0.50 MPa; (c) 1.00 MPa.

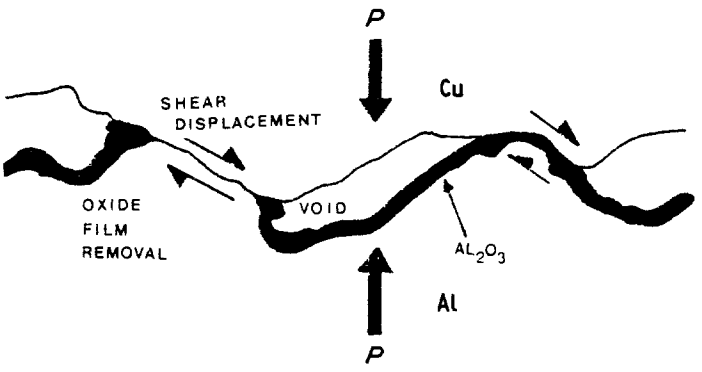


*Figure 4* Schematic diagram of the mechanisms of aluminium oxide film formation by shear displacements between microasperities in contact.

This can be observed by the increase in area where the phases or intermetallic compounds appear for the same bonding temperature (Figs 3a to c).

These first intermetallic nuclei were formed where the contact between areas of microroughness took place and plastic deformation was produced. The load application produced the breaking up of the oxide film at these contact points. This phenomenon can be explained by a mechanism similar to that proposed by Olson and Liby [8] for the diffusion bonding of beryllium: the oxide removal is produced by the shear displacements obtained between two microsperities in contact (Fig. 4).

However, pressure is the most important parameter at this stage, but surface roughness is also very important. A highly polished surface will reduce the shear displacements (Fig. 5). However, if the bonding surfaces are macroscopically rough, the bonded area is very limited and large voids are formed which are very difficult to suppress afterwards (Fig. 6).

When the joint is heated, there is a quick growth of the contact area due to creep. This phenomenon facilitates the previous mechanism.

However, at the end of this stage, the bonded area is less than 100% and many voids remain in the joint interface. These voids will be eliminated in the next stage of bond formation. The size and shape of these voids depends on the initial roughness.

### 3.1.2. Second stage

When the barriers that prevent intimate contact between the joining metals disappear, diffusive flows of matter begin across the bonding interface. This marks the beginning of the second stage of joint formation.

At this moment the interfacial voids have a lenticular shape with a low curvature ratio and their dimensions change between 0.5 and 10 $\mu$m high, and 5 and 30 $\mu$m long (Fig. 7).

The matter fluxes that act during the second stage produce two different but related phenomena: the shrinkage and spheroidization of some voids and the formation and growth of the first nuclei of intermetallic compounds (Figs 2c and d).

In Fig. 3a, the formation of one of these initial nuclei can be observed, in the contact point between two microasperities. These intermetallic compounds have been identified by EDS microanalysis as $Al_4Cu_9$ ($\tau_2$ phase) and $Al_2Cu$ ($\theta$ phase) (Table IV). In the corresponding BSE image, the (Al) and (Cu) solid solution can be observed (Fig. 8).

The quasi-spherical shape of these first nuclei (Fig. 9) confirms that the diffusive flows that are established during the second stage have a sink of matter, i.e. the neck formed in the contact zone between two areas of surface microroughness (Fig. 10). The proposed diffusional mechanisms are similar to those postulated by different authors to explain the sintering of metallic powders. For this reason, sintering principles can also be useful to explain the shape and size changes of the interfacial voids.

From Ashby's investigation [9] the mechanisms of matter transport which act in the second stage (Table V) can de deduced, the paths of which are represented in Fig. 11.

All these mechanisms have a common driving force:

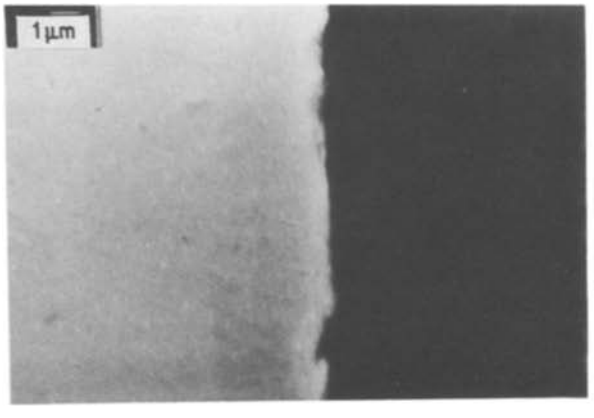


*Figure 5* Bond between two highly polished surfaces (0.5 $\mu$m) without the formation of an intermetallic compound ($T_s$ = 400° C, $t_s$ = 121 h and $P_s$ = 1.00 MPa).

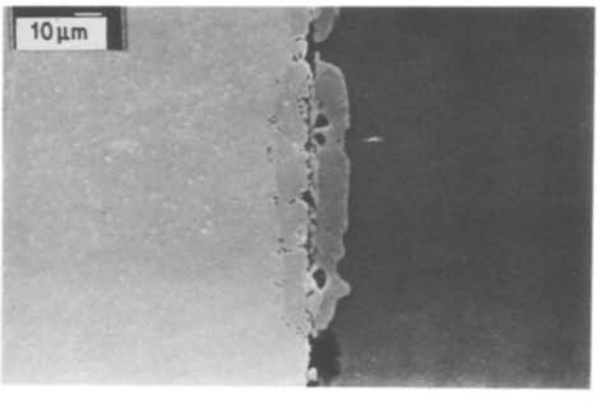


*Figure 6* Diffusion bond between two macroscopically rough surfaces with formation of large voids (> 5 $\mu$m) ($T_s$ = 400° C, $t_s$ = 42 h, $P_s$ = 1.00 MPa).

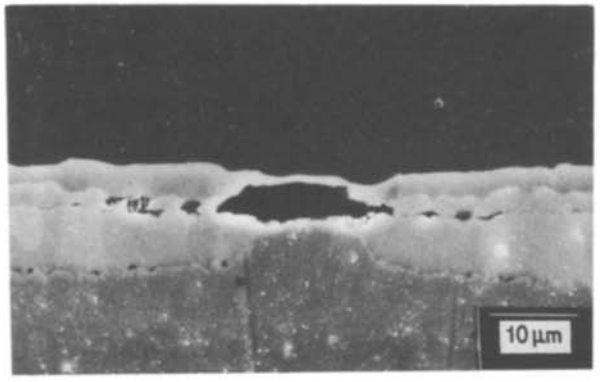


*Figure 7* Lenticular voids with high internal microroughness.

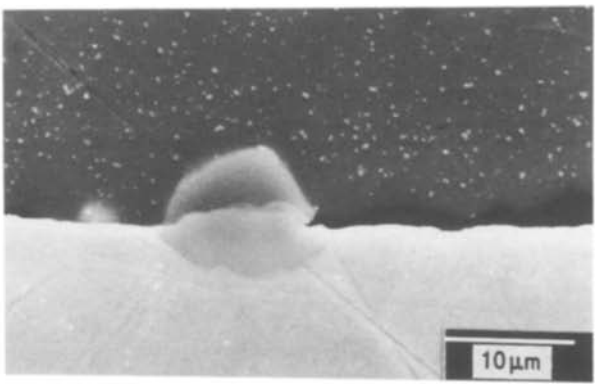


*Figure 9* The quasi-spherical shape of one intermetallic nucleus formed by $\theta$, $\eta_2$ and $\tau_2$ phases, growing in a neck between two microasperities.

the gradiant of chemical potential between the neck and other parts of the system, where the chemical potential is generally higher than that in the neck. This chemical potential depends on the surface curvature. For this reason the difference in surface curvature between sources and sink can be considered to be the driving force of these mechanisms.

On the other hand, all these mechanisms contribute to the neck growth and void spheroidization. But only certain of them lead to shrinkage or reduction of the relative volume of voids. This phenomenon is called "densification" in analogy to the sintering processes.

The surface mechanisms (first, second and third), only originate a change in the void shape, because they are limited to the transport of matter from certain zones of the void surface to the neck.

At the end of the second stage, the interfacial voids change their lenticular shape (Fig. 7) and become spherical (Fig. 12). This change originates an increase in the contact area and the driving forces of the surface mechanism are cancelled, so the flow of matter stops.

These diffusive mechanisms also originate the growth of the intermetallic compound nuclei and they join together to form continuous layers with the interfacial voids inside them (Figs 13a and b). During this growth, a third intermetallic compound appears inside the $\theta$ phase, which has been identified by EDS microanalysis as AlCu ($\eta_2$ phase) (Table IV).

### 3.1.3. Third stage

The third stage begins when the interfacial voids become spherical (Fig. 2e). Then the majority of the previous mechanisms stop, due to the annulment of their driving forces. However, the diffusion along the bond plane (interface diffusion) and the lattice diffusion (volume diffusion), with sources outside the voids, persist.

Both mechanisms produce several important phenomena. One is the shrinkage and elimination of the residual voids by matter flow from external sources (Fig. 14a to c). This flow can be considered as a couterflow of vacancies from the voids to the metal matrix.

Another important phenomenon that is produced during the third stage is the growth of the different intermetallic compound layers formed during the second stage. At this point, these layers develop a plain symmetry and grow parallel to the bond interface. During this growth, the layer of $\tau_2$ phase can cross the bond interface and surround it (Fig. 2f).

It has been observed in samples bonded at high temperature and for long times, that the bond interface may disappear by migration from the original bond plane in the same manner as boundary migration during normal grain growth. The driving force of these mechanisms is the reduction of the surface area, and thus the surface free energy of the system.

In the optical micrograph in Fig. 15 (taken using polarized light) of a sample submitted to thermal attack, some points where the original interface has

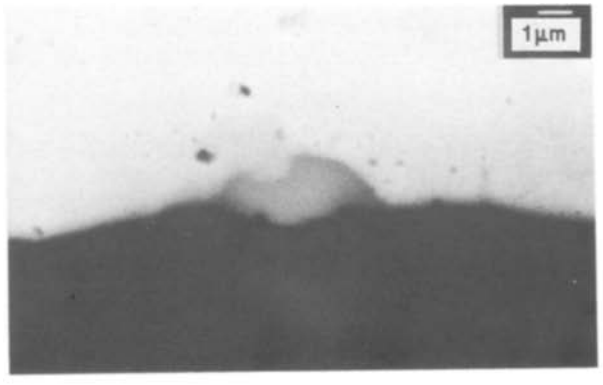


*Figure 8* BSE image of the nucleus shown in Fig. 3a. Aluminium and copper solid solutions are marked.

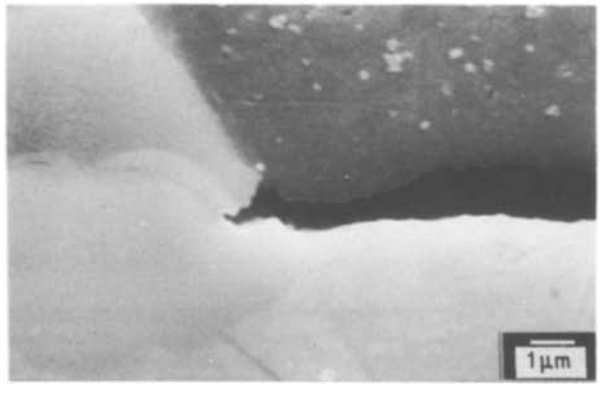


*Figure 10* Detail of the neck.

TABLE IV EDX microanalysis of the diffusion layers formed in the aluminium–copper joints

| Sample | No. of analyses | S.S. (Al) | | $\tau_2$ Phase | | $\eta_2$ Phase | | $\theta$ Phase | | S.S. (Cu) | |
|---|---|---|---|---|---|---|---|---|---|---|---|
| | | at % | dist. ($\mu$m) | at % | dist. ($\mu$m) | at % | dist. ($\mu$m) | at % | dist. ($\mu$m) | at % | dist. ($\mu$m) |
| M4 | 19 | 0.25 | 5 | 32.16 | 5 | 55.29 | 2 | 65.51 | 5 | 92.64 | 1 |
| | | 0.33 | 10 | 32.34 | 10 | 50.71 | 5 | 66.03 | 10 | 94.48 | 2 |
| | | 0.41 | 12 | 32.69 | 15 | | | 66.54 | 15 | 96.61 | 4 |
| | | 0.55 | 15 | | | | | 67.81 | 25 | 97.22 | 10 |
| | | | | | | | | 68.54 | 35 | 99.81 | 25 |
| | average % | | | 32.40 | | 50.50 | | 66.88 | | | |
| M7 | 20 | 0.35 | 5 | 32.32 | 5 | 50.25 | 2 | 66.16 | 5 | 93.55 | 1 |
| | | 0.58 | 8 | 32.41 | 10 | 50.82 | 5 | 66.83 | 10 | 94.66 | 2 |
| | | 0.73 | 10 | 32.64 | 15 | | | 67.03 | 15 | 95.84 | 5 |
| | | 0.91 | 15 | | | | | 67.36 | 25 | 97.16 | 10 |
| | | 0.99 | 18 | | | | | 68.44 | 35 | 99.41 | 25 |
| | average % | | | 32.46 | | 50.54 | | 67.16 | | | |
| M10 | 25 | 0.24 | 3 | 32.15 | 5 | 50.21 | 2 | 60.52 | 2 | 79.41 | 1 |
| | | 0.32 | 5 | 32.29 | 10 | 50.32 | 5 | 63.16 | 5 | 91.66 | 3 |
| | | 0.35 | 7 | 32.56 | 15 | 50.51 | 7 | 65.40 | 10 | 93.54 | 5 |
| | | 0.40 | 10 | 32.73 | 18 | | | 66.28 | 15 | 94.68 | 10 |
| | | 0.64 | 15 | | | | | 68.78 | 35 | 97.29 | 15 |
| | | 0.90 | 20 | | | | | 69.03 | 45 | 98.78 | 20 |
| | average % | | | 32.44 | | 50.35 | | 65.50 | | | |

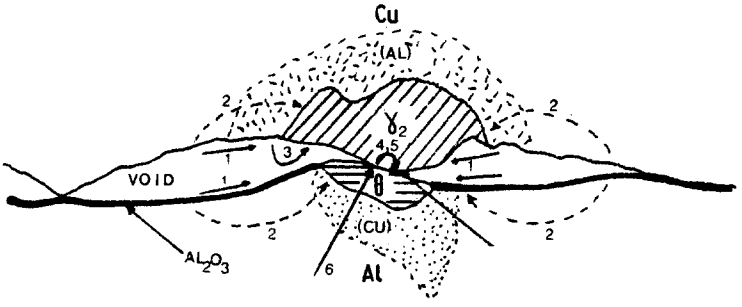


*Figure 11* Schematic representation of the diffusion mechanisms that act during the second stage of the bond formation.

disappeared due to the migration of the bond interface during the growth of the $\tau_2$ phase grains, can be observed. When this phenomenon occurs, the only mechanism that persists is the volume interdiffusion between copper and aluminium. For this reason, the phenomenon that occur after this are the slowest ones, and the elimination of the residual voids, now inside the $\tau_2$ grains, require high temperatures and long times.

## 4. Conclusions

This work has demonstrated that the metallographic study of dissimilar joints between metals that form intermetallic compounds can reveal considerable information which is of help in proposing a model of the process. It is evident that further work must study other important aspects such as the growth kinetics of the intermetallic compounds and the determination of diffusion coefficients in each intermetallic layers. However, the work reported here has shown the following significant points about the diffusion bonding of aluminium to copper.

1. A three-stage mechanistic model has been proposed to explain the formation of aluminium–copper diffusion-bonded joints.

2. The intermetallic compounds formed during diffusion bonding of aluminium to copper are $\tau_2$ ($Al_4Cu_9$), $\eta_2$ (AlCu) and $\theta$ ($Al_2Cu$).

3. The increase of bonding pressure during the first

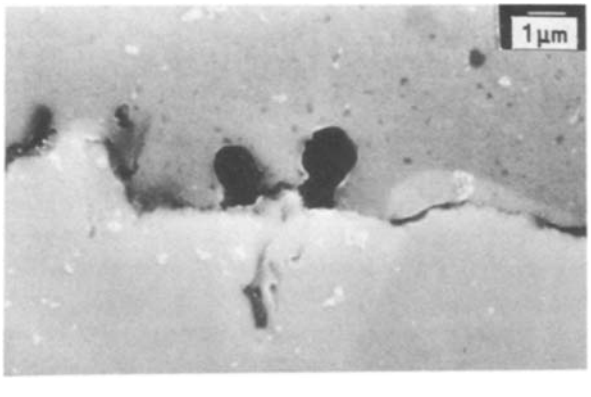


*Figure 12* Spherical voids between $\eta_2$ and $\tau_2$ phases.

TABLE V Diffusional mechanisms during the second stage of bond formation

| Mechanism no. | Transport path | Source of matter | Sink of matter |
|---|---|---|---|
| 1 | Void surface | Void surface | Neck |
| 2 | Metal lattice | Void surface | Neck |
| 3 | Vapour transport | Void surface | Neck |
| 4 | Bond interface | Bond interface | Neck |
| 5 | Metal lattice | Bond interface | Neck |
| 6 | Metal lattice | Metal lattice | Neck |

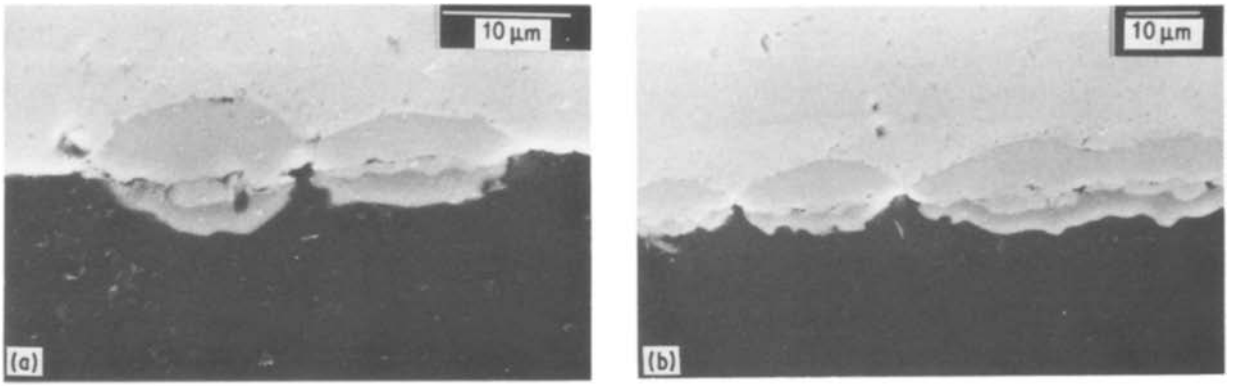


*Figure 13* Growth of the intermetallic compound nuclei to form a continuous layer. (a) $T_s$ = 520° C, $t_s$ = 15 min, $P_s$ = 1.60 MPa. (b) $T_s$ = 520° C, $t_s$ = 30 min, $P_s$ = 1.60 MPa.

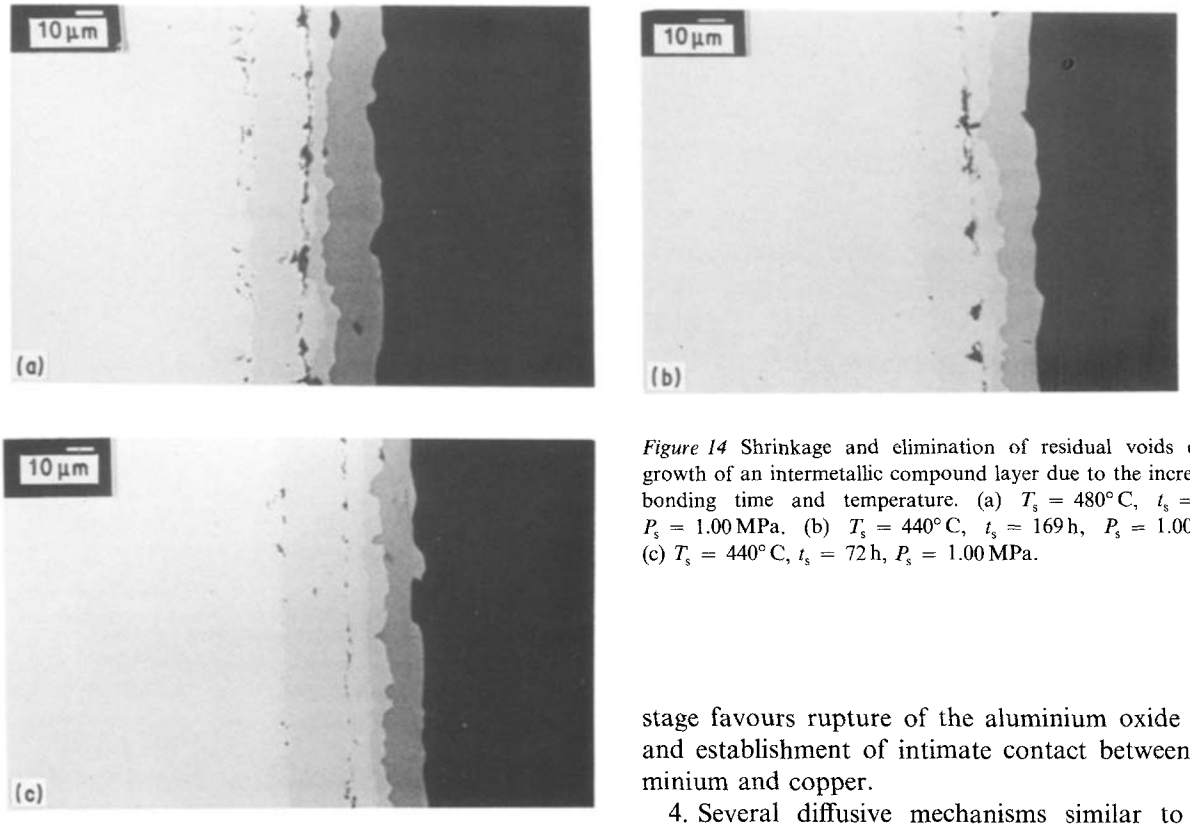


*Figure 14* Shrinkage and elimination of residual voids during growth of an intermetallic compound layer due to the increase of bonding time and temperature. (a) $T_s$ = 480° C, $t_s$ = 16 h, $P_s$ = 1.00 MPa. (b) $T_s$ = 440° C, $t_s$ = 169 h, $P_s$ = 1.00 MPa. (c) $T_s$ = 440° C, $t_s$ = 72 h, $P_s$ = 1.00 MPa.

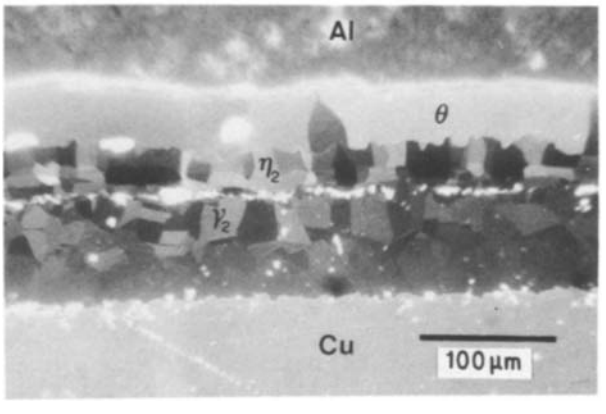


*Figure 15* Polarized light micrograph showing the disappearance of the original interface during the $\tau_2$ layer migration (thermal etching).

stage favours rupture of the aluminium oxide layer and establishment of intimate contact between aluminium and copper.

4. Several diffusive mechanisms similar to that proposed for sintering processes are dominant during the second stage. These mechanisms produced shrinkage and spheroidization of the interfacial voids and growth of the initial intermetallic nuclei to form a continuous layer.

5. During the third stage, the $\tau_2$ layer grows enclosing the original bond interface which can then disappear by a mechanism similar to normal grain growth

6. The elimination of the residual voids (intracrystalline voids) requires high temperatures and long times.

## References

1. J. L. MURRAY, *Inst. Met. Rev.* **30** (5) (1985) 211.
2. F. A. CALVO, A. UREÑA, J. M. GOMEZ DE SALAZAR and F. MOLLEDA, *J. Mater. Sci.*, to be published.
3. B. DERBY and E. R. WALLACH, *Met. Sci.* **16** (1982) 49.
4. W. H. KING and W. A. OWCZARSKI, *Weld. J.* **46** (1967) 289s.
5. G. GARMONG, N. E. PATON and A. S. ARGON, *Met. Trans. A* **6A** (1975) 1269.

6. P. M. BARTLE, "Information Package Series" (The Welding Institute, 1976) p. 1.
7. W. BRYANT, *Weld. J.* **54** (1975) 443s.
8. D. L. OLSON and A. L. LIBY, *Beryllium Sci. Technol.* **2** (1979) 275.
9. M. F. ASHBY, *Acta Metall.* **22** (1974) 275.

*Received 5 August*
*and accepted 22 October 1987*